Title
Dynamic Modeling and Simulation of Snowplow: Normal Operation and Icepack Impacts

Authors
Shou, Kun
Tomizuka, Masayoshi
Zhang, Wei-Bin

Publication Date
2000-12-01

CALIFORNIA PATH PROGRAM
INSTITUTE OF TRANSPORTATION STUDIES
UNIVERSITY OF CALIFORNIA, BERKELEY

Dynamic Modeling and Simulation of Snowplow: Normal Operation and Icepack Impacts

Kun Shou
Masayoshi Tomizuka
Wei-Bin Zhang

California PATH Research Report
UCB-ITS-PRR-2000-21

This work was performed as part of the California PATH Program of the University of California, in cooperation with the State of California Business, Transportation, and Housing Agency, Department of Transportation; and the United States Department of Transportation, Federal Highway Administration.

December 2000

ISSN 1055-1425

Dynamic Modeling and Simulation of Snowplow: Normal Operation and Icepack Impacts

Kun Zhou
Masayoshi Tomizuka
Department of Mechanical Engineering
University of California at Berkeley
Berkeley CA 94720

Wei-Bin Zhang
California PATH Headquarters
University of California at Berkeley
Richmond CA 94804

Abstract

In this report, three types of model pertaining to the normal operation and icepack impacts of snowplow are developed. First, a general method of deriving dynamic model for any snowplow with multi-blades is presented. This model includes all the nonlinear terms against existing dynamic models, which are derived under the assumption of small pitch motion and roll motion. With this model, the constraint forces and moments between the snowplow truck and the blades are obtained. Additionally, this modeling method is extended to a general method of deriving dynamic model for any multi-unit vehicles.

Secondly, a snow model is presented to estimate the casting forces, which act on the blades. It is shown that both of the lateral and longitudinal casting forces are proportional to v^2, where v is the traveling velocity of the snowplow truck.

Finally, an icepack-impact model is presented to simulate the dynamic performance of the snowplow under impact caused by the icepack. Several control techniques are applied to study the essential methods to minimize the hazardous consequences. It is shown that by changing the rear tire stiffness after impact, the yaw motion and the lateral motion of the snowplow can be remarkable reduced, and the time for the snowplow to set down to its steady-state is also half reduced. Additionally, with braking and steering control, the snowplow can be kept to remain on its own traveling path. It is also shown that, although the active automatic control will do a better job as expected, but in the case of no automatic control available, the driver himself still can control the snowplow to remain on its traveling path by taking brake and giving a suitable steering input to the snowplow truck. Several animations are made to show the effectiveness.

Keywords: Dynamic Modeling, Snowplows, Multi-Unit Vehicles, Icepack Impacts, Braking Control, Steering Control.

1. Introduction

Snowplow truck is an important facet of highway and road safety during winter season. Many articles have been written about dynamics of large trucks. But due to the dynamic loading of the snowplow by the blade, the dynamics of the snowplow truck are considerably different from that of a non-plowing truck.

This report focuses on developing a dynamic model of snowplow truck, developing a snow model to estimate the casting forces acting on the blade, and developing a icepack collision model to show the safety improvement by changing tire stiffness after collision.

The purposes of these models are:

- to study the interactions among the truck, the front blade, the snow and the road, and to provide useful information to improve the performance and reliability of the snowplow.
- to increase the safety and effectiveness of the snowplows.

Olson et al. (1995), using DADS (Dynamic Analysis and Design System), built a simulation model for a moldboard-equipped truck. Their snowplow model is presented by a truck with a blade, which is attached beneath the middle of the sprung mass of the truck. In this report, the snowplow truck with front blade is considered. The front blade is connected with the truck though a rigid frame. The rigid frame has a relative pitch motion with respect to the truck, and the blade has a relative yaw motion with respect to the frame. Hence the snowplow truck is a 3-unit vehicle. There are many articles about the dynamics of 2-unit tractor-semitrailer vehicles. Among them, Mikulcik (1968) used the Newtonian mechanics to derive the most complex model for the tractor-semitrailer. Chen (1996) used the lagrangian mechanics to derive a five-degree of freedom (translational motion, yaw motion and roll motion of the tractor, and the yaw of the semitrailer) complex model for the tractor-semitrailer. To our knowledge, there are few literatures on the dynamic model of general multi-unit vehicle. Tai (1998), under small pitch and roll motion assumption, used the Newtonian mechanics to derive a complex dynamic model for a class of general multi-unit vehicle.

Since the snowplow truck may be equipped with both the front and side blades to remove snow, the dynamics of the snowplow are considerably complicated due to the

dynamic loading carried by the two blades. The pitch motion and roll motion could be essential for fully understanding the dynamics of the snowplow. The assumption of small pitch and roll motion would not be valid anymore due to the complicated interaction between the snowplow and the road. Therefore, deriving a dynamic model of general multi-unit vehicle, which keeps all the nonlinear terms, becomes important to study the dynamic performance of the snowplow. On the other hand, deriving the equation of motion for multi-unit vehicle is the most difficult part in modeling. A structured-modeling-method is desired to be developed, which would make the modeling person's job as easy as possible, while leave the difficult part to the powerful computers. In Section 2, a new dynamic model for general multi-unit vehicle is presented using Newtonian mechanics.

For one way blade plow, which casts the snow to one side, there is an acute-angle between the casting direction and the driving direction. Hence there is a lateral force acting on the blade. This will affect the lateral and yaw motions of the snowplow. In Section 3, a snow model is presented to estimate the casting forces.

Interviews with the drivers show that one of the most dangerous cases in operating the snowplow is the collision with an icepack on the outer-side of the blade. The snowplow will spin around and slide away from the traveling path after the collision, and threaten the safety of its driver and other drivers on the adjacent road. In order to investigate potential approaches for mitigating the impact due to icepack, a simple icepack collision model is developed. Simulation results are presented in Section 4 to show the safety improvement by using several control techniques, including increasing the rear tire stiffness after impact, steering control and braking control, etc.

2. Dynamic model of general multi-unit vehicle

2.1 Coordinate systems

Each unit of the multi-unit vehicle is treated as a rigid body with mass concentrated at the C.G. In order to facilitate the description of the dynamics of the general multi-unit vehicle, several coordinate systems are used in modeling process. For each unit, there are

an unsprung mass coordinate system $\{\vec{e}_u\}$ and a sprung mass coordinate system $\{\vec{e}_s\}$. The $\{\vec{e}_s\}$ frame is attached to the unit with the origin at C.G., with $\vec{e}_s^{\,1}$, $\vec{e}_s^{\,2}$ and $\vec{e}_s^{\,3}$ on the longitudinal, lateral and upward directions, respectively. The $\{\vec{e}_u\}$ frame is the projection of $\{\vec{e}_s\}$ on the road surface. $\{\vec{e}_s\}$ and $\{\vec{e}_u\}$ are moving frames. And $\{\vec{E}\}$ is a globally fixed inertial reference coordinate. The relation of these coordinates is shown as following.

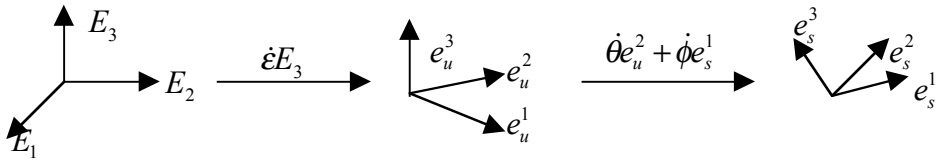

Fig. 1 Relation among the three coordinate systems

where ε, θ and ϕ are the yaw angle, pitch angle and the roll angle, respectively.

2.2 Single unit vehicle

Before moving to the modeling of multi-unit vehicle, let's consider single unit vehicle first.

The kinematics of the single unit vehicle are

$$\begin{aligned} \vec{v} &= v_x\vec{e}_u^{\,1} + v_y\vec{e}_u^{\,2} + v_z\vec{e}_u^{\,3} = \begin{pmatrix} v_x & v_y & v_z \end{pmatrix}\{\vec{e}_u\} \\ \vec{\omega} &= \dot{\varepsilon}\vec{E}_3 + \dot{\theta}\vec{e}_u^{\,2} + \dot{\phi}\vec{e}_s^{\,1} = \begin{pmatrix} \omega_1 & \omega_2 & \omega_3 \end{pmatrix}\{\vec{e}_s\} \end{aligned} \tag{1}$$

and the equations of motion are

$$\begin{aligned} \frac{d}{dt}(M\vec{v}) &= \vec{F}^e \\ \frac{d}{dt}(J\vec{\omega}) &= \vec{M}^e \end{aligned} \tag{2}$$

where M is the mass and $J = \begin{pmatrix} J_1 & J_2 & J_3 \end{pmatrix}\{\vec{e}_s\}$ is the tenser of mass moment of inertial of the vehicle. $\vec{F}^e = \begin{pmatrix} F_1^e & F_2^e & F_3^e \end{pmatrix}\{\vec{e}_u\}$ and $\vec{M}^e = \begin{pmatrix} M_1^e & M_2^e & M_3^e \end{pmatrix}\{\vec{e}_s\}$ are the external forces and external moment acting on the vehicle, respectively. Then,

$$
\begin{aligned}
M\begin{pmatrix} \dot{v}_x - \dot{\varepsilon} v_y \\ \dot{v}_y + \dot{\varepsilon} v_x \\ \dot{v}_z \end{pmatrix} &= \begin{pmatrix} F_1^e \\ F_2^e \\ F_3^e \end{pmatrix} \\
\begin{pmatrix} J_1\dot{\omega}_1 + (J_3 - J_2)\omega_2\omega_3 \\ J_2\dot{\omega}_{21} + (J_1 - J_3)\omega_1\omega_3 \\ J_3\dot{\omega}_3 + (J_2 - J_1)\omega_1\omega_2 \end{pmatrix} &= \begin{pmatrix} M_1^e \\ M_2^e \\ M_3^e \end{pmatrix}
\end{aligned} \tag{3}
$$

To solve this set of equations, in most of the references, the state variables are selected as v_x, v_y, v_z, ε, θ, ϕ and $\dot{\varepsilon}$, $\dot{\theta}$, $\dot{\phi}$. From equation (1), we have

$$
\begin{bmatrix} \omega_1 \\ \omega_2 \\ \omega_3 \end{bmatrix} = \begin{bmatrix} 1 & 0 & -\sin\theta \\ 0 & \cos\phi & \sin\phi\cos\theta \\ 0 & -\sin\phi & \cos\phi\cos\theta \end{bmatrix} \begin{bmatrix} \dot{\phi} \\ \dot{\theta} \\ \dot{\varepsilon} \end{bmatrix} \tag{4}
$$

Substituting equation (4) into equation (3), we can obtain the equations of motion in terms of this set of state variables.

However, since the Jacobian of the transform (4) is $\dfrac{\partial(\omega_1 \quad \omega_2 \quad \omega_3)}{\partial(\phi \quad \dot{\theta} \quad \dot{\varepsilon})} = \cos\theta$, which is nonsingular in driving condition, equation (4) can be inverted as

$$
\begin{bmatrix} \dot{\phi} \\ \dot{\theta} \\ \dot{\varepsilon} \end{bmatrix} = \begin{bmatrix} 1 & \tan\theta\sin\phi & \tan\theta\cos\phi \\ 0 & \cos\phi & -\sin\phi \\ 0 & \sin\phi\sec\theta & \cos\phi\sec\theta \end{bmatrix} \begin{bmatrix} \omega_1 \\ \omega_2 \\ \omega_3 \end{bmatrix} \tag{5}
$$

Now, by selecting the state variables as v_x, v_y, v_z, ε, θ, ϕ and ω_1, ω_2, ω_3, equations (3) and (5) are already in the standard form. The advantages of this selecting of state variables are:

1) The calculation of derivatives is avoided, which is considered as the toughest part of deriving the equations of the motion.
2) $\bar{\omega}$ has distinct physical meaning and is easier to be measured than $\dot{\varepsilon}$, $\dot{\theta}$ and $\dot{\phi}$.
3) This method is easy to be extended for multi-unit vehicles, and to develop a structured-modeling-method.

2.3 Two-unit vehicle

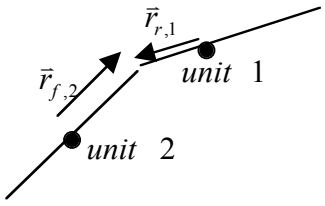

Hereafter, the parameters with subscript *i* describe the i^{th} unit.

The equations of motion of two-unit vehicle are

$$\begin{aligned}
\frac{d}{dt}(M\vec{v})_1 &= \vec{F}_1^{\,e} + \vec{F}^c \\
\frac{d}{dt}(J\vec{\omega})_1 &= \vec{M}_1^{\,e} + \vec{M}^c + \vec{r}_{r,1} \times \vec{F}^c \\
\frac{d}{dt}(M\vec{v})_2 &= \vec{F}_2^{\,e} - \vec{F}^c \\
\frac{d}{dt}(J\vec{\omega})_2 &= \vec{M}_2^{\,e} - \vec{M}^c - \vec{r}_{f,2} \times \vec{F}^c
\end{aligned} \tag{6}$$

$$\begin{bmatrix} \dot{\phi} \\ \dot{\theta} \\ \dot{\varepsilon} \end{bmatrix}_i = \begin{bmatrix} 1 & \tan\theta\sin\phi & \tan\theta\cos\phi \\ 0 & \cos\phi & -\sin\phi \\ 0 & \sin\phi\sec\theta & \cos\phi\sec\theta \end{bmatrix}_i \begin{bmatrix} \omega_1 \\ \omega_2 \\ \omega_3 \end{bmatrix}_i \qquad i = 1,2 \tag{7}$$

where $\vec{F}^c$ and $\vec{M}^c$ are the constraint force vector and the constraint moment vector acting on the connection point between unit 1 and 2. $\vec{r}_{r,i}$ and $\vec{r}_{f,i}$ are the position vectors directed from the C.G. of the i^{th} unit to the rear and the front connection points, respectively.

However, equation (6) and (7) are not independent, and some constraint conditions at the connection point must be specified.

2.3.1 Constraints at the connection point

Two basic assumptions are:

1) There is no relative translation motion between unit 1 and 2 at the connection point, i.e.,

$$\vec{v}_2 = \vec{v}_1 + \vec{w}_1 \times \vec{r}_{r,1} - \vec{w}_2 \times \vec{r}_{f,2} \tag{8}$$

thus the constraint force vector acting on the connection point has three non-zero components.

2) There is only one relative rotational motion between two units at the connection point. Three typical cases are

- relative yaw motion, i.e.,

$$\bar{\omega}_2 = \bar{\omega}_1 + \dot{\varepsilon}_f \vec{e}_s^3 \tag{9}$$

- relative pitch motion, i.e.,

$$\bar{\omega}_2 = \bar{\omega}_1 + \dot{\varepsilon}_f \vec{e}_s^2 \tag{10}$$

- relative roll motion, i.e.,

$$\bar{\omega}_2 = \bar{\omega}_1 + \dot{\varepsilon}_f \vec{e}_s^1 \tag{11}$$

where ε_f describes the relative rotational motion.

The constraint moment vector acting on the connection point has two non-zero components.

2.3.2 Geometric relations

Intuitively, if we know the kinematics of the first unit and those of ε_f and $\dot{\varepsilon}_f$, the kinematics of the second unit can be obtained. In this section, the geometric relations between these two units are derived.

Considering, in the first case, two units having relative yaw motion. The transform matrix from the coordinate system $\{\vec{e}_s\}_1$ to $\{\vec{e}_s\}_2$ is given by

$$\left[\{e_s\}_1 \rightarrow \{e_s\}_2\right] = \begin{bmatrix} \cos\varepsilon_f & \sin\varepsilon_f & 0 \\ -\sin\varepsilon_f & \cos\varepsilon_f & 0 \\ 0 & 0 & 1 \end{bmatrix} \tag{12}$$

and that from $\{\vec{e}_s\}_i$ to $\{\vec{e}_u\}_i$ is given as follows

$$\left[\{e_s\}_i \rightarrow \{e_u\}_i\right] = \begin{bmatrix} \cos\theta & \sin\theta\sin\phi & \sin\theta\cos\phi \\ 0 & \cos\phi & -\sin\phi \\ -\sin\theta & \cos\theta\sin\phi & \cos\theta\cos\phi \end{bmatrix}_i \qquad i = 1,2 \tag{13}$$

The transform matrix from $\{\vec{e}_u\}_1$ to $\{\vec{e}_u\}_2$ can be obtained from (12) and (13) as

$$\left[\{e_u\}_1 \to \{e_u\}_2\right] = \left[\{e_u\}_1 \to \{e_s\}_1\right] \times \left[\{e_s\}_1 \to \{e_s\}_2\right] \times \left[\{e_s\}_2 \to \{e_u\}_2\right] \tag{14}$$

On the other hand, according the definition of the coordinate systems, we have

$$\left[\{e_u\}_1 \to \{e_u\}_2\right] = \begin{bmatrix} \cos(\varepsilon_2 - \varepsilon_1) & \sin(\varepsilon_2 - \varepsilon_1) & 0 \\ -\sin(\varepsilon_2 - \varepsilon_1) & \cos(\varepsilon_2 - \varepsilon_1) & 0 \\ 0 & 0 & 1 \end{bmatrix} \tag{15}$$

Combining equation (14) and (15), we have

$$\begin{aligned} &\begin{bmatrix} \cos\theta_2 & \sin\theta_2 \sin\phi_2 & \sin\theta_2 \cos\phi_2 \\ 0 & \cos\phi_2 & -\sin\phi_2 \\ -\sin\theta_2 & \cos\theta_2 \sin\phi_2 & \cos\theta_2 \cos\phi_2 \end{bmatrix} \begin{bmatrix} \cos\varepsilon_f & \sin\varepsilon_f & 0 \\ -\sin\varepsilon_f & \cos\varepsilon_f & 0 \\ 0 & 0 & 1 \end{bmatrix} \\ &= \begin{bmatrix} \cos(\varepsilon_2 - \varepsilon_1) & \sin(\varepsilon_2 - \varepsilon_1) & 0 \\ -\sin(\varepsilon_2 - \varepsilon_1) & \cos(\varepsilon_2 - \varepsilon_1) & 0 \\ 0 & 0 & 1 \end{bmatrix} \begin{bmatrix} \cos\theta_1 & \sin\theta_1 \sin\phi_1 & \sin\theta_1 \cos\phi_1 \\ 0 & \cos\phi_1 & -\sin\phi_1 \\ -\sin\theta_1 & \cos\theta_1 \sin\phi_1 & \cos\theta_1 \cos\phi_1 \end{bmatrix} \end{aligned} \tag{16}$$

Hence, if the two units have relative yaw motion, i.e., $\vec{\omega}_2 = \vec{\omega}_1 + \dot{\varepsilon}_f \vec{e}_s^{\,3}$, then θ_2, ϕ_2 and ε_2 can be solved in terms of θ_2, ϕ_2, ε_2 and ε_f as

$$\begin{aligned} \sin\theta_2 &= \sin\theta_1 \cos\varepsilon_f - \cos\theta_1 \sin\phi_1 \sin\varepsilon_f \\ \tan\phi_2 &= \tan\phi_1 \cos\varepsilon_f + \tan\theta_1 \sec\phi_1 \sin\varepsilon_f \\ \sin(\varepsilon_2 - \varepsilon_1) &= \cos\phi_2 \sec\theta_1 \sin\varepsilon_f \end{aligned} \tag{17}$$

Similarly, if the two units have relative pitch motion, i.e., $\vec{\omega}_2 = \vec{\omega}_1 + \dot{\varepsilon}_f \vec{e}_s^{\,2}$, then

$$\begin{aligned} \sin\theta_2 &= \sin\theta_1 \cos\varepsilon_f - \cos\theta_1 \cos\phi_1 \cos\varepsilon_f \\ \tan^{-1}\phi_2 &= \tan^{-1}\phi_1 \cos\varepsilon_f + \tan\theta_1 \csc\phi_1 \sin\varepsilon_f \\ \sin(\varepsilon_2 - \varepsilon_1) &= -\sin\phi_2 \sec\theta_1 \sin\varepsilon_f \end{aligned} \tag{18}$$

And, if the two units have relative roll motion, i.e., $\vec{\omega}_2 = \vec{\omega}_1 + \dot{\varepsilon}_f \vec{e}_s^{\,1}$, then

$$\begin{aligned} \theta_2 &= \theta_1 \\ \varepsilon_2 &= \varepsilon_1 \\ \phi_2 &= \phi_1 + \varepsilon_f \end{aligned} \tag{19}$$

2.3.3 Equations of motion of two unit vehicle

Substituting the constraint conditions (8), (9)~(11), and the geometry relations (17)~(19) into equations (6) and (7), we have the following independent equations of motion of two unit vehicle:

$$\frac{d}{dt}(M\vec{v})_1 = M_1\begin{pmatrix}\dot{v}_x - \dot{\varepsilon}v_y\\ \dot{v}_y + \dot{\varepsilon}v_x\\ \dot{v}_z\end{pmatrix}_1\{\vec{e}_u\}_1 = \vec{F}_1^{\,e} + \vec{F}^c$$

$$\frac{d}{dt}(J\vec{\omega})_1 = \begin{pmatrix}J_1\dot{\omega}_1 + (J_3 - J_2)\omega_2\omega_3\\ J_2\dot{\omega}_{21} + (J_1 - J_3)\omega_1\omega_3\\ J_3\dot{\omega}_3 + (J_2 - J_1)\omega_1\omega_2\end{pmatrix}_1\{\vec{e}_s\}_1 = \vec{M}_1^{\,e} + \vec{M}^c + \vec{r}_{r,1}\times\vec{F}^c \qquad (20)$$

$$\begin{bmatrix}\dot{\phi}\\ \dot{\theta}\\ \dot{\varepsilon}\end{bmatrix}_1 = \begin{bmatrix}1 & \tan\theta\sin\phi & \tan\theta\cos\phi\\ 0 & \cos\phi & -\sin\phi\\ 0 & \sin\phi\sec\theta & \cos\phi\sec\theta\end{bmatrix}_1\begin{bmatrix}\omega_1\\ \omega_2\\ \omega_3\end{bmatrix}_1$$

$$\frac{d}{dt}(M\vec{v})_2 = \vec{F}_2^{\,e} - \vec{F}^c$$

$$\frac{d}{dt}(J\vec{\omega})_2 = \vec{M}_2^{\,e} - \vec{M}^c - \vec{r}_{f,2}\times\vec{F}^c$$

where $\vec{v}_2$ and $\vec{\omega}_2$ are given in equations (9)~(11) with respect to different connection conditions. Solving equation (20) with applied forces, moments and initial conditions, the 16 unknown $\vec{v}_1(3)$, $\vec{\omega}_1(3)$, ϕ, θ, ε, ε_f, $\dot{\varepsilon}_f$, $\vec{F}^c(3)$ and $\vec{M}^c$ (2) can be obtained. Here, $\vec{v}_1(3)$ denotes that the vector $\vec{v}_1$ has three components.

2.3.4 A brief summary on modeling for two unit vehicle

There are several characters of the dynamic model described above:

1) There is no small roll, pitch motion assumption. All nonlinear terms are included.
2) The workload of deriving the equations of motion is remarkably reduced. For example, when the two units have relative yaw motion, according to equations (8) and (9), we have $\vec{v}_2 = \vec{v}_1 + \vec{w}_1\times\vec{r}_{r,1} - \vec{w}_2\times\vec{r}_{f,2}$ and $\vec{\omega}_2 = \vec{\omega}_1 + \dot{\varepsilon}_f\vec{e}_s^{\,3}$. Hence

$$\dot{\vec{v}}_2 = \dot{\vec{v}}_1 + \dot{\vec{\omega}}_1\times\vec{r}_{r,1} + \vec{\omega}_1\times\vec{\omega}_1\times\vec{r}_{r,1} - \dot{\vec{\omega}}_2\times\vec{r}_{f,2} - \vec{\omega}_2\times\vec{\omega}_2\times\vec{r}_{f,2} \qquad (21)$$

and

$$\dot{\vec{\omega}}_2 = \dot{\vec{\omega}}_1 + \ddot{\varepsilon}_f \vec{e}_s^3 + \dot{\varepsilon}_f \vec{\omega}_1 \times \vec{e}_s^3 \tag{22}$$

i.e., the derivatives of $\vec{v}_2$ and $\vec{\omega}_2$ can be directly obtained in terms of the state variables, and the tough work of derivative calculation is avoided. Also, a small subroutine can be made to calculate the vector cross product ($\times$), hence keep all equations in vector form.

3) For each unit *i*, the Newton equation is described in the coordinate system $\{\vec{e}_u\}_i$, while the Euler equation is described in $\{\vec{e}_s\}_i$. To apply the connection conditions, the transform matrixes of $[\{\vec{e}_u\}_i \to \{\vec{e}_s\}_i]$ ($i=1, 2$), $[\{\vec{e}_u\}_1 \to \{\vec{e}_u\}_2]$ are needed. These transform matrixes are given in equations (12) ~ (15).
4) The constraint forces and moments can be obtained along with the kinematics of the two-unit vehicle. The force information is very useful, which can help the maintenance of the snowplow, and reduce the cost.
5) The same idea can be easily extended to a general multi-unit vehicle, and form a structured-modeling-method.

2.4 Multi-Unit vehicle

Considering the typical i^{th} and $(i+1)^{th}$ units of a general multi-unit vehicle. Similar as that in Section 2.3.3, the equations of motion for these two units are

$$\begin{aligned}
\frac{d}{dt}(M\vec{v})_i &= \vec{F}_i^e + \vec{F}_{r,i}^c + \vec{F}_{f,i}^c \\
\frac{d}{dt}(J\vec{\omega})_i &= \vec{M}_i^e + \vec{M}_{r,i}^c + \vec{M}_{f,i}^c + \vec{r}_{r,i} \times \vec{F}_{r,i}^c + \vec{r}_{f,i} \times \vec{F}_{f,i}^c \\
\frac{d}{dt}(M\vec{v})_{i+1} &= \vec{F}_{i+1}^e + \vec{F}_{r,i+1}^c + \vec{F}_{f,i+1}^c \\
\frac{d}{dt}(J\vec{\omega})_{i+1} &= \vec{M}_{i+1}^e + \vec{M}_{r,i+1}^c + \vec{M}_{f,i+1}^c + \vec{r}_{r,i+1} \times \vec{F}_{r,i+1}^c + \vec{r}_{f,i+1} \times \vec{F}_{f,i+1}^c
\end{aligned} \tag{23}$$

where $\vec{F}^c_{r,i}$, $\vec{M}^c_{r,i}$ are the constraint force vector and the constraint moment vector acting on the rear side connection point of unit *i,* and $\vec{F}^c_{f,i}$, $\vec{M}^c_{f,i}$ are those on the front side connection point. Thus $\vec{F}^c_{r,i} = -\vec{F}^c_{f,i+1}$, $\vec{M}^c_{r,i} = -\vec{M}^c_{f,i+1}$.

To understand that the above modeling method is actually a structural-method, assuming that the equations of motion for the first *i* units have been obtained without considering the $(i+1)^{th}$ unit. Here, the $(i+1)^{th}$ unit could be connected with any unit in the first *i* units, say the j^{th} unit. The connection point can be anywhere, i.e., not necessarily at the front or rear side of the unit. Let $\vec{r}_1$ be the position vector from the C.G. of the j^{th} unit to the connection point between $(i+1)^{th}$ and j^{th} units, and $\vec{r}_2$ is the position vector from the C.G. of the $(i+1)^{th}$ unit to the same connection point. To add the $(i+1)^{th}$ unit into the system, we only need to add $\vec{F}^c_{i+1,j}$ and $\vec{M}^c_{i+1,j} + \vec{r}_1 \times \vec{F}^c_{i+1,j}$ to the right hand sides of the Newton and Euler's equations of the j^{th} unit, respectively. And then add additional equations

$$\begin{aligned} \frac{d}{dt}(M\vec{v})_{i+1} &= \vec{F}^e_{i+1} - \vec{F}^c_{i+1,j} \\ \frac{d}{dt}(J\vec{\omega})_{i+1} &= \vec{M}^e_{i+1} - \vec{M}^c_{i+1,j} - \vec{r}_2 \times \vec{F}^c_{i+1,j} \end{aligned} \tag{24}$$

to form a new set of equations of motion for the *i+1* unit system. If the $(i+1)^{th}$ unit and the j^{th} unit have relative yaw motion, similar as equations (21) and (22), we have

$$\begin{aligned} \vec{v}_{i+1} &= \vec{v}_j + \vec{w}_j \times \vec{r}_1 - \vec{w}_{i+1} \times \vec{r}_2 \\ \dot{\vec{v}}_{i+1} &= \dot{\vec{v}}_j + \dot{\vec{\omega}}_j \times \vec{r}_1 + \vec{\omega}_j \times \vec{\omega}_j \times \vec{r}_1 - \dot{\vec{\omega}}_{i+1} \times \vec{r}_2 - \vec{\omega}_{i+1} \times \vec{\omega}_{i+1} \times \vec{r}_2 \end{aligned} \tag{25}$$

and

$$\begin{aligned} \vec{\omega}_{i+1} &= \vec{\omega}_j + \dot{\varepsilon}_{f,i+1,j} \vec{e}^3_{s,j} \\ \dot{\vec{\omega}}_{i+1} &= \dot{\vec{\omega}}_j + \ddot{\varepsilon}_{f,i+1,j} \vec{e}^3_{s,j} + \dot{\varepsilon}_{f,i+1,j} \vec{\omega}_j \times \vec{e}^3_{s,j} \end{aligned} \tag{26}$$

Similarly, the equations for the relative pitch and/or roll motion between the $(i+1)^{th}$ unit and the j^{th} unit can be obtained as those in Section 2.3. The transform matrixes from the coordinate systems defined on the $(i+1)^{th}$ unit to those on the j^{th} unit are the same as equations (12)~(15).

Given the geometric configuration of a general multi-unit vehicle system, using the method described above, the full set of equations of motion can be obtained by "combining" several subsystems together. Hence this is a structural-modeling-method.

2.5 Modeling of snowplow

As mentioned in Section 1, the snowplow with front blade is modeled as a three-unit vehicle, with the truck, the frame and the blade as the unit 1, 2 and 3, respectively. Using the method described above, a dynamic model of snowplow has been developed.

For the snowplow with both front and side blades, the snowplow is modeled as a four-unit vehicle system in which the first three units are the same as those described above, and the 4^{th} unit is the side blade, which has relative yaw motion with respect to the truck.

For unit 1, the applied (external) force $\vec{F}_i^e$ is the sum of the tire forces. For unit 3 or 4, $\vec{F}_i^e$ is the sum of snow-casting forces and friction forces between the blade and the road. The vector $\vec{M}_i^e$ is the moment caused by $\vec{F}_i^e$ with respect to the C.G. of the i^{th} unit.

Since the snowplows are operated on an icy surface during winter season, and most of the time they work with chains on tires, therefore the tire model, especially the tire with chains, is an important issue for snowplow modeling. To fully understand the dynamic performance of the snowplow, a good tire model for snowplow need to be developed. This could be one of the main issues in subsequent phases. In this report, an ideal nonlinear tire model has been used to describe the tire-road interactions (see Section 4.2).

3 Snow model and casting forces

In service conditions, the snow is cast to one side. There is an acute angle between the casting direction and the traveling direction, which would cause a remarkable lateral casing force acting on the blade, and hence affect the lateral motion and the yaw motion of the snowplow. A snow model needs to be developed to estimate the casting forces.

Nixon et al. (1997) operated serials of field tests to measure the ice scraping forces on the snowplow with underbody blade. And the effectiveness of different types of cutting edges for scraping ice has also been studied. Minsk (1981) introduced a snow model for a snowplow with a wedge plow, and the estimated casting forces have been obtained for this model. In this report, independently but with the similar mathematical analysis, a snow model for a snowplow with a cylindrical plow has been developed, and the formulas for estimating the casting forces are obtained.

The geometry of the plow is modeled as partial of a cylinder with ratio R . (see Fig. 2).

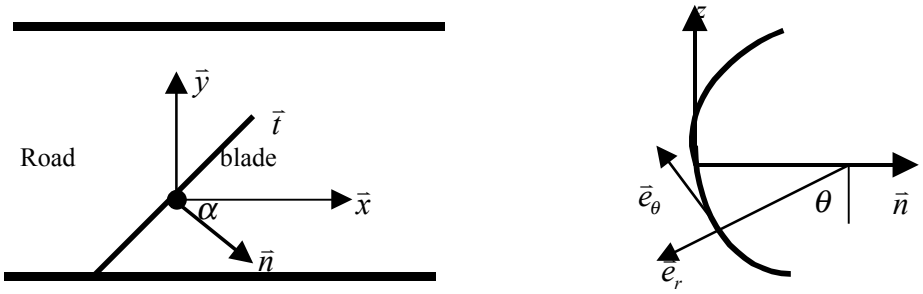

Fig. 2 Geometry of the blade

where $\{\vec{x} \quad \vec{y} \quad \vec{z}\}$ is the road coordinate system with respect to the longitudinal, lateral and upward directions, respectively. $\{\vec{n} \quad \vec{t} \quad \vec{z}\}$ is the following coordinates fixed on the blade, with $\vec{n}$ refers to the casting direction. α is the angle between the traveling direction ($\vec{x}$) and the casting direction ($\vec{n}$).

The basic assumptions of the snow model are:

- The friction between the snow and the blade is small and can be neglected.
- There is no compaction of the snow in service conditions.

Under these assumptions, the absolute value of the relative velocity of the snow sheets with respect to the blade equals to the absolute value of the velocity of the truck. Let $\vec{v}_{truck} = v\vec{x}$, then the relative velocity of the snow sheets with respect to the blade is

$$\vec{v}_r = v[(-\sin\alpha)\vec{t} + (\cos\alpha)\vec{e}_\theta] \tag{27}$$

where

$$\vec{e}_\theta = \sin\theta\vec{z} - \cos\theta\vec{n} \tag{28}$$

Hence the absolute velocity of the snow sheet is

$$\begin{aligned}\vec{v}_{snow} &= \vec{v}_{truck} + \vec{v}_r \\ &= v\left(\cos^2\alpha(1-\cos\theta)\vec{x} - \sin\alpha\cos\alpha(1-\cos\theta)\vec{y} + \cos\alpha\sin\theta\vec{z}\right)\end{aligned} \tag{29}$$

The change in the momentum of the snow sheet is caused by the casting forces. According to Newton's law, we have

$$\vec{F}\Delta t = -m\vec{v}_{snow} = -(\rho A v\Delta t)\vec{v}_{snow} \tag{30}$$

where ρ is the density of the snow, and $A = HL$ is the crossing-section area of the snow sheet with H as the depth of the snow being cast, and L as the width of the cut blade.

Thus the casting forces acting on the blade are given as follows

$$\vec{F} = F_x\vec{x} + F_y\vec{y} + F_z\vec{z} \tag{31}$$

where

$$\begin{aligned}F_x &= -\rho A v^2\cos^2\alpha(1-\cos\theta) \\ F_y &= \rho A v^2\sin\alpha\cos\alpha(1-\cos\theta) \\ F_z &= -\rho A v^2\cos\alpha\sin\theta\end{aligned}$$

But, during high speed ploughing (over 30miles/hour), the snow sheet probably does not behave in the ideal manner which satisfies the assumptions mentioned before. Especially, the compression of snow becomes evident and should be considered in snow modeling. Several references studied more complex snow models. For example, Kempainen et al. (1998) studied a complex model, which includes the compressive, shear and turbulent zones in front of the blade. They suggested that a fluid snow model might be necessary to describe the high speed ploughing.

4 Icepack collision model and simulations

Interviews with the drivers show that the collision with the icepack occurs at least once during each service season. Due to the large impact forces, the snowplow will spin, and slid away from its driving path, and might collide with other vehicles on the adjacent road. It is well know that braking is dangerous when the vehicle has large yaw motion, and the experienced drivers just do nothing when the icepack impact occurs. The drivers require a way that can mitigate the impact due to the icepack. The objective of this

icepack collision model analysis is to investigate potential approaches to minimize the hazardous consequences.

To simulate the icepack collision, a simple dynamic model for the snowplow has been developed under the following assumptions:

- The pitch, roll and bouncing motions are small, and can be neglected.
- The applied (external) forces acting on the snowplow come from the tire forces and the casting forces.
- Tire model is an ideal nonlinear model.

4.1 Geometric configuration of the snowplow and input parameters

The geometry configuration of icepack collision is shown in Fig. 3.

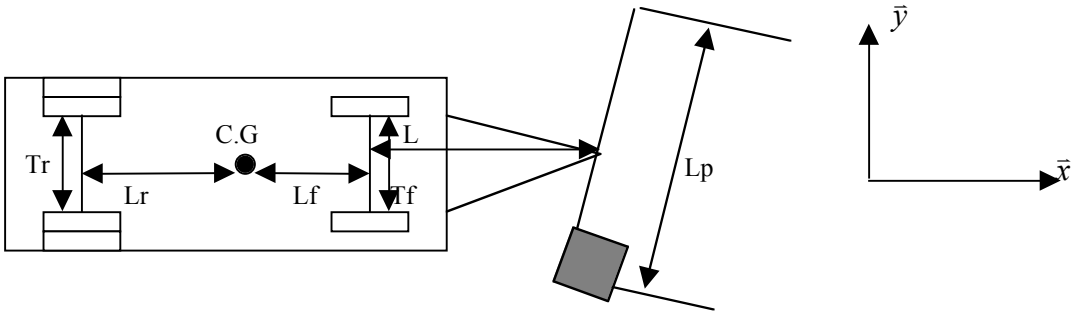

Fig. 3 Geometry configuration

The parameters used in the collision model are given in Table 1.

Parameter	Unit	Value	Description
m	Kg	16252	Mass of the vehicle
I_z	$Kg-m^2$	132111	Moment of inertia about vertical axis
L_f	m	2.2	Distance between CG and front wheel axle
L_r	m	2.5	Distance between CG and rear wheel axle
T_f	m	2.12	Front wheel axle width
T_r	m	2.12	Rear wheel axle width
L	M	2.0	Distance between the front axle and the C.G. of the blade
L_p	m	3.0	Plow width

$C_{\alpha f}$	N/rad	143330	Cornering stiffness of front wheel
$C_{\alpha r}$	N/rad	80312	Cornering stiffness of rear wheel
v_x	m/s		Unsprung mass longitudinal velocity
v_y	m/s		Unsprung mass lateral velocity
ε	rad		Yaw angle
$\dot{\varepsilon}$	rad/s		Yaw rate
Fx	N		Longitudinal force
Fy	N		Lateral force
Mz	N-m		Moment about vertical axis
α_f	rad		Slip angle of the front wheel
α_r	rad		Slip angle of the rear wheel
α_{cri}	rad		Critical slip angle
δ	rad		Steering angle

Table 1. Definition and values of parameters

4.2 Nonlinear tire model

Due to the collision, the yaw motion of the snowplow is large, therefore the linear tire model is insufficient to describe the motion of the snowplow. Here, an ideal nonlinear tire model is used. For each tire, the relation between the lateral force F_y and the tire slip angle is shown in Fig. 4.

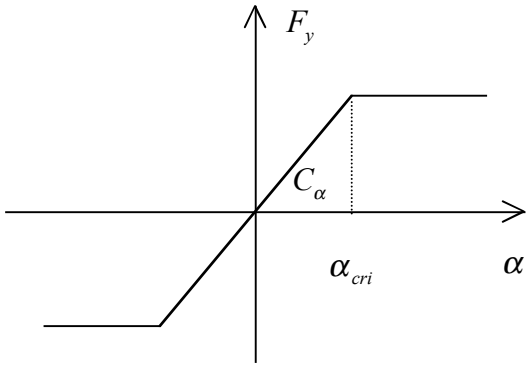

Fig. 4 Ideally nonlinear tire model

i.e.,

$$F_y = \begin{cases} C_\alpha \cdot \alpha & if\ |\alpha| < \alpha_{cri} \\ C_\alpha \cdot \alpha_{cri} & otherwise \end{cases} \tag{32}$$

4.3 Simulation results and analysis

Using the ideal nonlinear tire model and the simple vehicle dynamic model mentioned above, sets of simulations have been done.

In simulation, the icepack collision is modeled as a very large impulse compact force acting on the right outer-side of the blade as shown in Fig. 5.

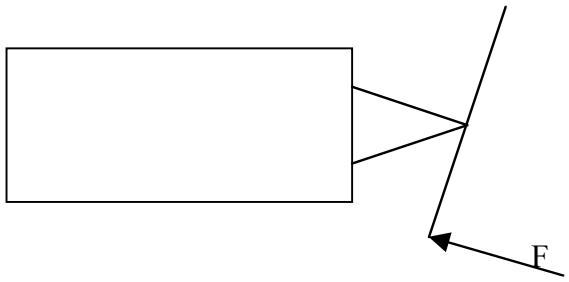

Fig. 5 Icepack collision model

In order to investigate the potential methods for mitigating the impact due to icepack, we assume that the cornering stiffness of the tires can be changed by someway after collision occurs. Intuitively, if we can increase the rear tire stiffness, the corresponding lateral forces provided by the tires would restrict the yaw motion and lateral motions of the snowplow, and therefore improve the safety. Examples for ways of changing tire stiffness could be spreading sand or other materials locally around the tire, (the snowplows are fully loaded with sand in service conditions), or changing the tire pressure.

Simulation was conducted to compare the behaviors of the snowplow with and without changing of the rear tire stiffness. In both cases, the truck travels with a velocity of 25 miles/hour before the collision. The original critical slip angle of the rear tires is $\alpha_{cri} = 6^{\circ}$. For the case of changing tire stiffness, the critical slip angle was changed to $\alpha_{cri} = 9^{\circ}$ with a 0.1-second's time-delay after detecting the collision.

In our first simulation, we assume that for both cases (with and without changing tire stiffness), the drive does not take any action after impact. The results are shown in Fig. 6.

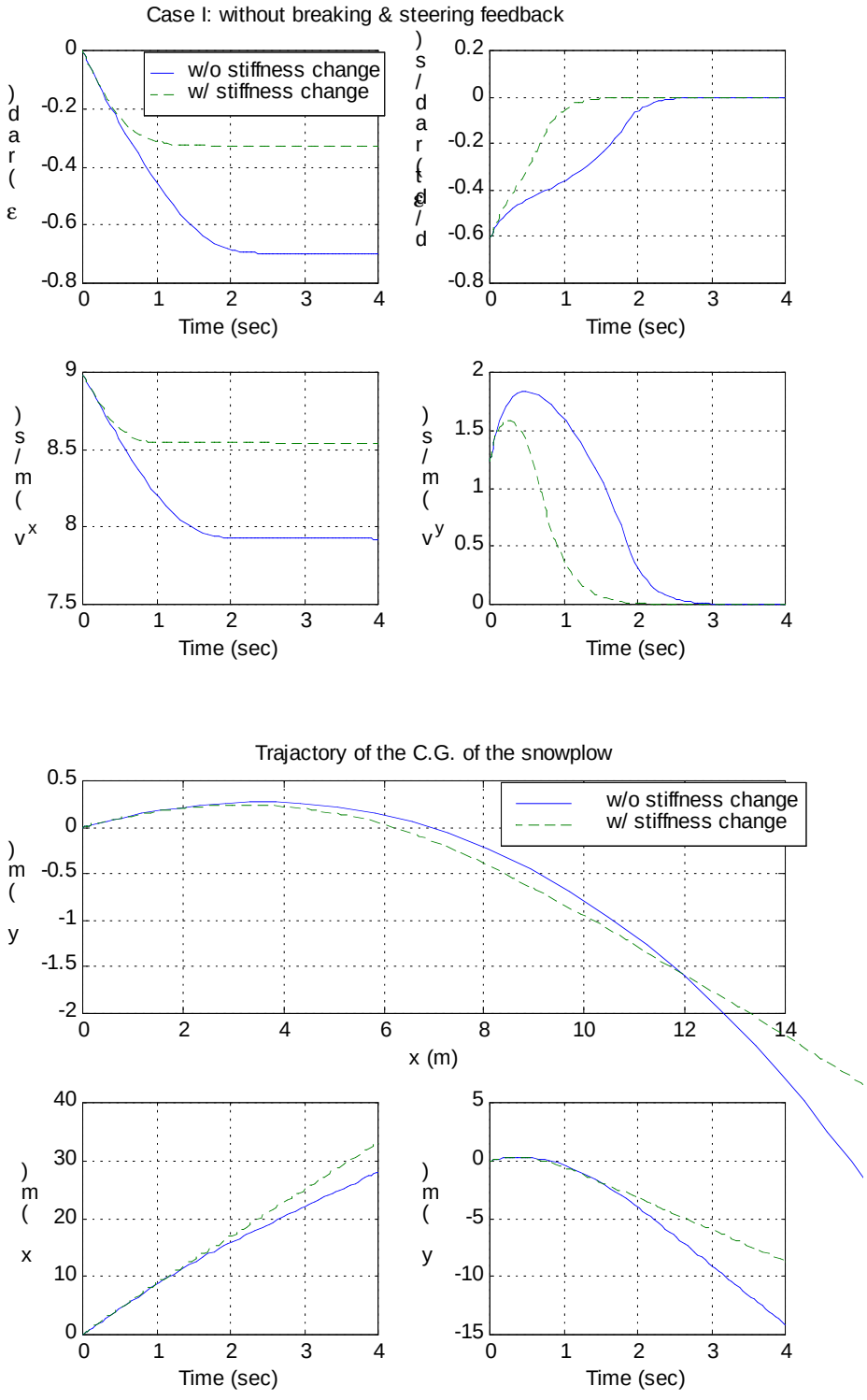

Fig. 6 Case I: Simulation results of without braking and steering feedback

In Fig. 6, ε and $\dot{\varepsilon}$ denote the yaw angle and yaw rate, respectively. v_x and v_y refer to the longitudinal and lateral velocities of the snowplow. *x* and *y* are the fixed inertial coordinates, with *x* pointing to the traveling direction. The collision occurs at *t=0*.

The simulation results show that a notable reduction of the yaw and lateral motions of the snowplow can be achieved by increasing the stiffness of the rear tires. On the other hand, even though the difference for the maximum lateral sliding distances between the two cases are small, but the time period that the snowplow staying in adjacent road is remarkably reduced (nearly a half). This can be clearly shown in the icepack collision animations. The other important issue that must be pointed out is that the setting time (the time for the snowplow to set down to its steady state after impact) for the case of increasing rear tire stiffness is about only a half of that of without changing tire stiffness. This is a crucial improvement, it saves time for the driver to apply brake or other more complex control techniques to stop the snowplow safely.

It is also noticed that the dynamics of the snowplow can be improved by decreasing the stiffness of the front tires. But the effect was not as efficient as increasing the stiffness of the rear tires.

Note that the tire stiffness is changed after the collision occurs, it is reasonable for the snowplow to still slid away from its traveling path. If a sensor system can be equipped at the front of the blade to detect the icepack, more remarkable improvement could be expected to be achieved.

However, as we can see, if the driver do not apply brake after the snowplow has been set down, the snowplow will travel towards its right adjacent lane, and hence put other vehicles on that road in danger.

In our second set of simulation, the driver applies brake with a time delay of *t* seconds after detecting the icepack impact. Since the yaw motion is remarkable reduced after the tire stiffness is changed, it saves time for the driver to apply brake safely. The time delay is chosen as $t = 0.4s$ and $t = 0.8s$, respectively, for the cases of changing tire stiffness and without change tire stiffness. The simulation results are shown in Fig. 7.

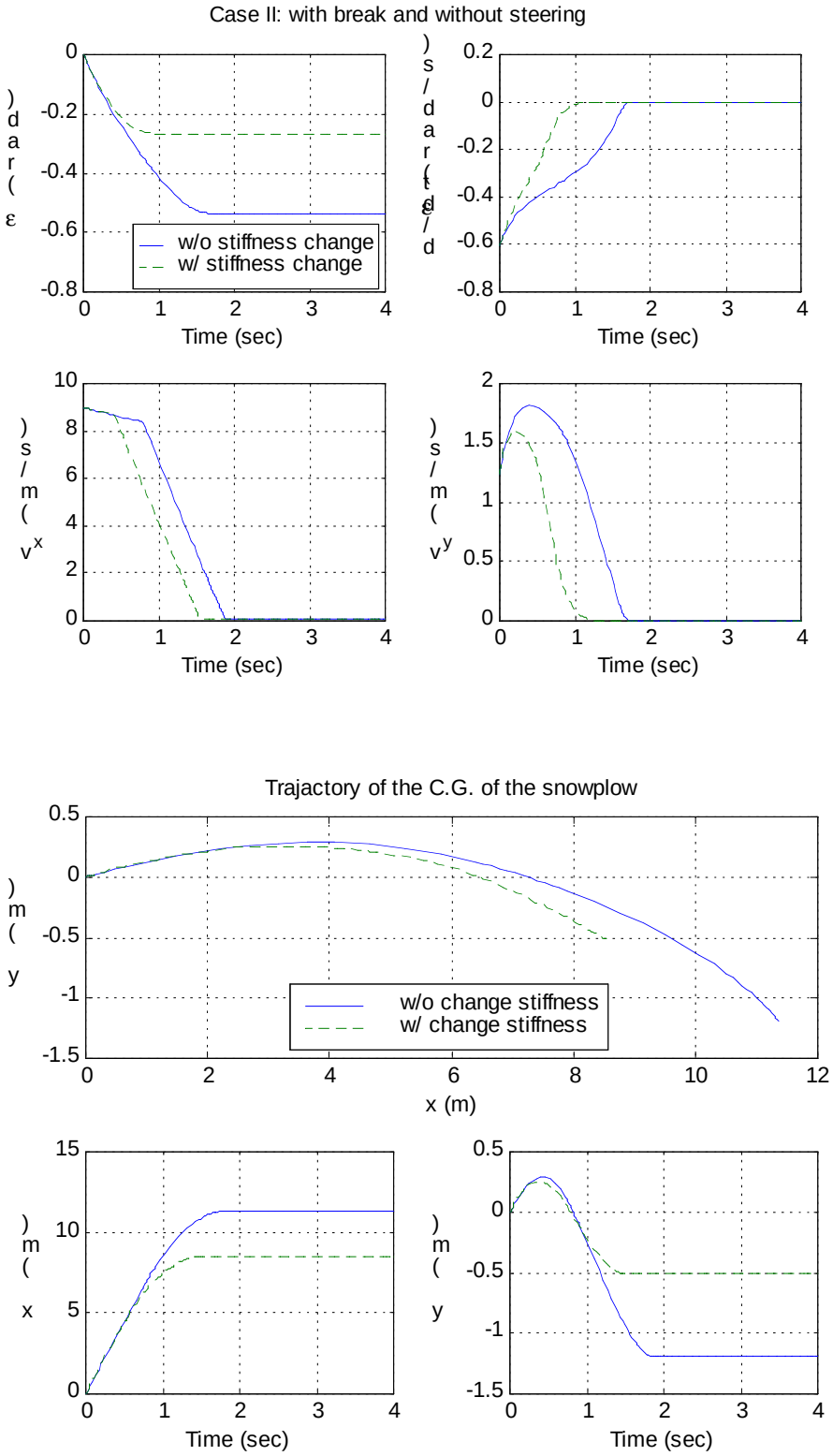

Fig. 7 Simulation results of snowplow with brake and without steering input

As we expected, by changing tire stiffness, the operation of the snowplow is safer than that without changing tire stiffness. However, the snowplow still would merge to its right adjacent road. To control the snowplow stops on its road center, the steering input is needed. In the following simulation, a steering input $\delta = -\varepsilon$ is applied to the case of changing tire stiffness, with a time delay $t = 0.4s$ after icepack impact. For the case of without changing tire stiffness, the steering input will make the situation worse.

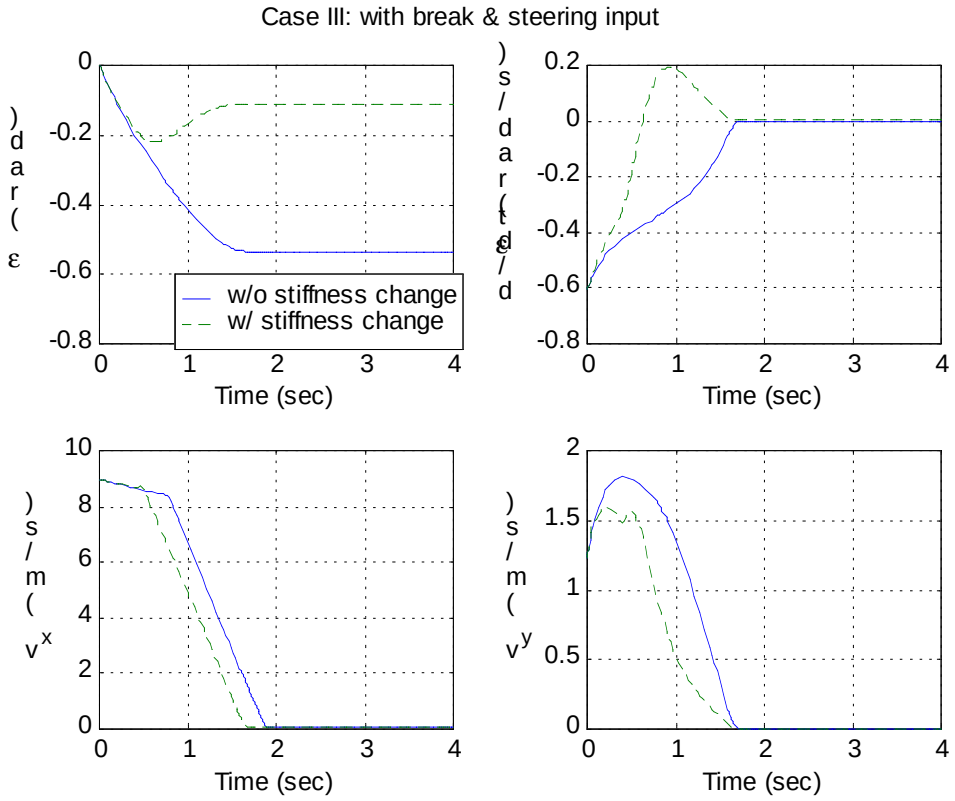

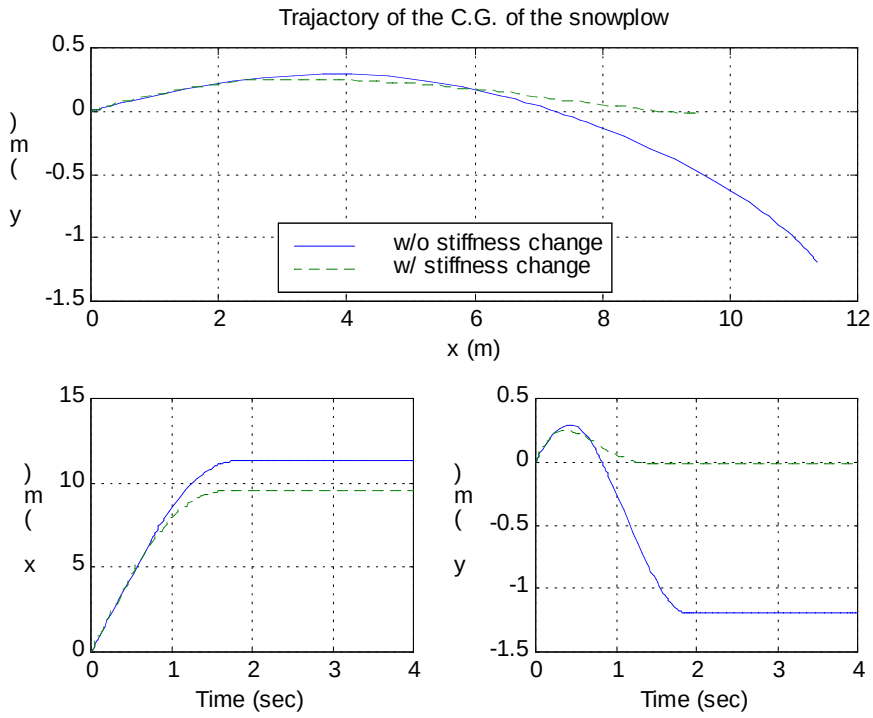

Fig. 8 Simulation results of snowplow with brake and active steering input

The simulation results show that with brake and active steering feedback, the snowplow can be controlled to stop with its C.G. right on its center of road, and $\varepsilon = -0.1rad$, which guarantees the whole body of the snowplow would remain in its travelling road. In simulation, the steering input depends on the active yaw angle of the snowplow, therefore it is difficult to ask the driver to give the right steering input. To study whether there is a way that the driver, who does not know the yaw angle of the snowplow on line, can control the snowplow to remain on its travelling road, a steady steering input $\delta = 0.2rad$, instead of active steering feedback $\delta = -\varepsilon$, is applied in the following simulation with a time delay $t = 0.4s$ after the impact. The results are shown in Fig. 9.

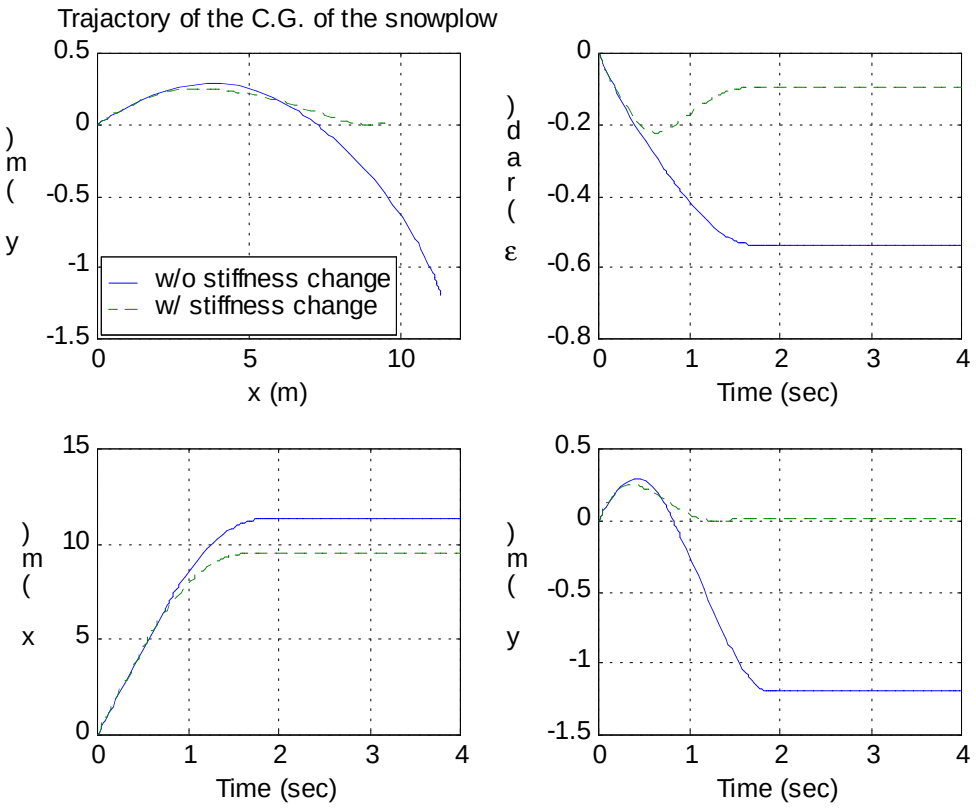

Fig. 9 Simulation results of snowplow with brake & stead steering input

Hence, after changing tire stiffness, the driver himself still can control the snowplow efficiently by braking and giving a suitable steady steering input and keep the snowplow remaining on its road. This is an important result, which shows that, before further studies of active automatic control techniques, there is an efficient way that can be operated by the driver to mitigate the impact due to icepack.

4.4 A brief summary of analysis of collision simulation results

From the simulation results shown in the previous Section, we can conclude that

- By increasing the rear tire stiffness after impact caused by icepack, the yaw and lateral motion can be reduced remarkable. Thus save time to apply active control, and also save time for the driver himself to apply steady steering input.

- With benefit of changing tire stiffness, the active steering feedback control and brake control can be applied to guarantee that the snowplow would remain on its travelling path.
- In the case of without knowing the yaw angle on line or with no active control available, there is a potential way that the driver can control the snowplow remains on its road, with brake and a suitable steady steering input.
- Further improvement can be expected if more complicated active control techniques, such as sliding control, etc., are applied.

5. Animations

Based on the models developed in this report, two sets of animations have been made by Dr. Khorramabad. With the data of the snow motion, which is obtained from the snow model mentioned in Section 3, the first set of animations shows the casting process of the snowplow serviced in a straight road. The second set of animation shows the comparison for the dynamics of the snowplow between with and without changing the tire stiffness after icepack impact.

In the second set of animations, the snowplow is in service with a velocity *30 miles/hour*, while in adjacent left road (which is clean, no snow), a passenger car is traveling in the same direction with velocity a velocity of *45 miles/hour*. At the time that the icepack collision occurs, the passenger car is *84m* behind the snowplow. With a 0.8-second's delay, the driver of the passenger car takes brake to decease its velocity, the decreasing acceleration is $9m/s^2$.

- Case 1: the passenger car takes brake until full stop, while the snowplow is operated without changing of tire stiffness.
- Case 2: the passenger car takes brake until full stop, while the snowplow is operated with tire stiffness being changed.
- Case 3: the passenger car takes a half brake until its traveling speed becomes a half of its original speed (i.e., *22.5 miles/hour*), and keep going with the reduced speed, while the snowplow is operated with tire stiffness being changed.

It is shown that the passenger car nearly crashes with the snowplow in case 1, while it is safely stopped in case 2. It even safely travels through the road in case 3, but it is impossible for the case that the tire stiffness does not change.

6. Conclusions

In this report, a structural dynamic model for the snowplow was presented. There is no assumption of small pitch and roll motion in this dynamic model, therefore all the nonlinear terms are included. With this model, it is able to study whether the pitch motion and the roll motion could play an important role in the normal operation of the snowplow and safety improvement. Also, this structural-modeling-method can be easily extended to a general modeling method for multi-unit vehicles, which is an interesting subject of Automatic Highway System (AHS). Any snowplow with multi-blades can be modeled by the proposed method. As an example, the dynamic model of a snowplow with a front blade was presented.

A simple but basic snow model was presented. The casting forces acting on the blade are important to study the normal operation of snowplow. With the proposed snow model, the formula of calculating the casting forces were presented. Based on this snow model, further more complex snow model could be developed.

An icepack-impact model was presented to investigate the potential methods of improving the safety with the impact caused by icepack. The simulation results show that the yaw motion and the lateral motion of the snowplow can be remarkably reduced by increasing the rear tire stiffness after impact. Also, the setting time (the time for the snowplow to set down to its steady state after impact) for the case of increasing the rear tire stiffness is only about a half of that of without changing tire stiffness. This gives us valuable time to apply braking control and steering control to keep the snowplow remaining on its traveling path. More important, the simulation shows that even with no active automatic control available, the driver himself still can keep the snowplow remaining on its own traveling path by taking brake and giving a suitable steering input. Based on the simulation data, two sets of animations were made to show the effectiveness.

References

[1] Olson, W. W. et al., *Dynamic Model of A Truck Equipped with An Underbody Mid-mounted Snowplow Blade,* Michigan Technological University, Houghton, Michigan, 49931 Final Report No. GLCTTR 68-95/01, 1995.

[2] Mikulcik, E. C., *The Dynamics of Tractor-Semitrailer Vehicles: The Jackkinfing Problem,* Ph.D. Thesis, Cornell University, Ithaca, N.Y., 1968.

[3] Chen, C., *Backstepping Design of Nonlinear Systems and Its Application to Vehicle Lateral Control in Automated Highway Systems,* Ph.D. Thesis, UC Berkeley, CA, 1996.

[4] Tai, M., *Dynamic Modeling of Multi-unit Heavy Vehicles*, California PATH Research Report, UCB-ITS-PRR-98-8, 1998.

[5] Nixon, W.A. et al, *Measurement of Ice Scraping Forces on Snowplow Underbody Blades,* IIHR Technical Report No. 385, 1997.

[6] Minsk, L.D., *Snow Removal Equipment,* Handbook of Snow, edit by D.M. Grey and D.H. Male, Pergamon Press Canada Ltd., Toronto, 1981.

[7] Kempainen, A. et al, *Modeling and testing snow ploughing forces on trucks,* Int. J. of Vehicle Design, Vol. 19, No. 4, 1998.